RESEARCH REPORT RR-021

SPHERICAL HARMONIC ANALYSIS OF THE NORMAL CONSTANT PRESSURE CHARTS IN THE NORTHERN HEMISPHERE

by

S. T. AWADE, G. C. ASNANI & R. N. KESHAVAMURTY

INDIAN INSTITUTE OF TROPICAL METEOROLOGY

Ramdurg House
Ganeshkhind Road
Poona-5, India

May 1978

SPHERICAL HARMONIC ANALYSIS OF THE NORMAL CONSTANT PRESSURE CHARTS IN THE NORTHERN HEMISPHERE

RR-24

By

S.T. Awade, G.C. Asnani and R.N. Keshavamurty
Indian Institute of Tropical Meteorology, Poona - 5.

Abstract :

It is believed that the large scale anomalies in the performance of the Indian summer monsoon are a part of the general circulation anomalies having periods larger than the four monsoon months. It may, therefore, be possible to link anomalies of the Indian summer monsoon with anomalies of the global flow pattern, a few months ahead. To get anomalies of global flow pattern, we need quantitative measures of normal global flow pattern.

With this idea in view, the monthly northern hemispheric constant pressure charts prepared by Free University of Berlin have been subjected to spherical harmonic analysis for m = 0, 1, 2, ---, 18 and n - m = 0, 2, 4, ---, 18.

The features of normal contour patterns for the

... 2

months of March to July are presented in this report for n - 1, 2 and n - m = 0, 2 for standard isobaric levels 850, 700, 500, 300, 200 and 100 mb. The vertical and the horizontal tilts of wave numbers 1 and 2 are discussed in some detail.

2. Introduction :

India's economy very much depends on the monsoon. Naturally, ever since the inception of India meteorological department nearly a century ago, there has been a demand for long range forecasting of the summer monsoon, a couple of months in advance if possible.

It stands to reason that anomalies in the monsoon activity which have horizontal extent of the Indian region and are persistant for a few months should be part of the phenomenon which is global in extent and has a period of at least half to one year. In the beginning of this century when only surface meteorological observations were available, it was natural to think in terms of lag correlation coefficient between pressure and rainfall recorded a few months earlier at a few selected surface observatories scattered over the globe and the subsequent monsoon activity over India. This work of correlation was started by Walker (24) and has been in practice in India

... 3

for several years. For a history of this technique and its present status, the reader is referred to Rao (20), Jagannathan (12) and Raghavendra and Roberts (19).

Now, we have upper air observations. Also there has been better understanding and appreciation of the dynamics of the monsoon and its relationship to the global circulation. Hence one would like to examine the upper air data to see the evolution of the global circulation before the onset of the monsoon and during its stay over the country. With this aim in view, we now have in the Indian Institute of Tropical Meteorology, a project of diagnostic study to find out if there are significant anomalies in large scale global flow pattern before and during the summer monsoon which could be dynamically connected to the anomalies (departures from normal) in the subsequent behaviour of the monsoon. For this, we need convenient quantitative measures of normal large scale flow patterns.

We confined our analysis to the northern hemisphere rather than to the entire earth sphere, because the density of data is far better in the northern hemisphere than in the southern hemisphere. This disparity in the density of data is well recognised (Eliasen, et al (6)). At present, we have fairly

... 4

dependable normal geopotential charts prepared by the Free University of Berlin (8) based on the data for the years 1951-60. We used these charts for the analysis.

On the spherical earth surface, the spherical harmonics constitute the most natural set of orthogonal functions for the study of planetary scale meteorological systems. Haurwitz (10) was perhaps the first who utilised the spherical harmonics in the theory of large scale meteorological systems. Blinova (3) developed the theory further in terms of spherical harmonics. Craig (4) gave the solution of nonlinear verticity equation in terms of these functions and Neamtan (17) improved upon that solution.

Haurwitz and Craig (11) fitted the spherical harmonics to the actual meteorological data and showed that such an analysis offers a powerfull method of representing a large amount of meteorological data in terms of relatively few numbers and thus could become a useful tool in climatological and dynamical meteorology. Subsequently, the technique of spherical harmonics has been applied in the field of meteorology by several authors (Silberman, (22); Kubota, (15); Platzman, (18); Baer, (1); (2); Ellsaesser, (7); Saltzman, (21); Merilees, (16)).

... 5

It was decided to represent in terms of the spherical harmonics, the geopotential field of the normal and the actual charts for the standard isobaric levels 850, 700, 500, 300, 200 and 100 mb.

A comparison between the normal and the actual charts for the extremely abnormal monsoon season of 1972 has already been reported by Keshavamurty and Awade (13). Similar comparison is in progress for other years also and will be reported in course of time.

The purpose of this paper is to present the principal features of the normal charts for the months March to July to cover the period of three months (March to May) before the onset of monsoon, one month (June) of advance and establishment of the monsoon over India and one month (July) when the monsoon is in peak activity over the country.

2. Method :

The Salient features of the method adopted are given below. The justification for these steps is given in Eliasen and Machenhauer (6).

i] Symmetry was assumed across the equator.

ii] Along the latitude circle Ø, the height was taken as

... 6

$$H(\lambda) = \sum_{m=0}^{\infty} (a_m(\phi) \operatorname{Cos} m\lambda + b_m(\phi) \operatorname{Sin} m\lambda) \quad \ldots (1)$$

By conventional Fourier analysis, we obtained the truncated series

$$\left.\begin{aligned} H(\lambda) &= \sum_{m=0}^{18} A_m(\phi) \operatorname{Cos} m\lambda + B_m(\phi) \operatorname{Sin} m\lambda \\ R_m &= \sqrt{A_m^2 + B_m^2}, \quad \tan\epsilon = \frac{B_m}{A_m} \end{aligned}\right\} \quad \ldots (1a)$$

iii) On the sphere, the field is given by

$$H(\phi, \lambda) = \sum_{m=0}^{\infty} \sum_{n=m}^{\infty} \left(a_n^m \operatorname{Cos} m\lambda + b_n^m \operatorname{Sin} m\lambda \right) p_n^m(\mu) \quad \ldots (2)$$

where $p_n^m(\mu)$ is the associated Legendre function of the first kind, m is the number of waves along a latitude circle and (n-m) is the number of nodal points between the north pole and south pole, excluding the poles themselves. μ is equal to Sin ϕ. Due to the restriction of the analysis to the northern hemisphere and due to the assumption of symmetry across the equator, the orthogonality condition for the Legendre polynomial becomes

$$\int_0^1 p_n^m(\mu)\, p_{n'}^m(\mu)\, d\mu = 0 \text{ and } n + n' \text{ even}, \quad n \neq n' \quad \ldots (3)$$

(n-m) is an even integer .... (4)

The normalisation condition is

$$\int_0^1 (p_n^m(\mu))^2 \, d\mu = 1 \quad \ldots (5)$$

... 7

(iv) The coefficients a_n^m and b_n^m are given by

$$a_n^m = \int_0^1 a_m (\phi) \; p_n^m (\mu) \; d\mu \qquad \ldots (6)$$

$$b_n^m = \int_0^1 b_m (\phi) \; p_n^m (\mu) \; d\mu \qquad \ldots (7)$$

(v) The amplitude R_n^m and the phase δ are given by

$$R_n^m = \sqrt{(a_n^m)^2 + (b_n^m)^2} \qquad \ldots (8)$$

and $$\tan \delta = \frac{b_n^m}{a_n^m} \qquad \ldots (9)$$

The data from the Free University of Berlin normal charts (8) were picked at interval of 5 degree longitude and 5 degree latitude from the equator to the north pole for the levels mentioned above. The spherical surface harmonics were fitted to the data for range m = 0 to 18 and (n≠m) = 0 to 18 by the least square method.

3. Result of spherical harmonic analysis :

The normal geopotential height was analysed for each of the six constant pressure surfaces and for each

... 8

of the five months, for m = 0 , 1, 2, --, 18 and (n-m) = 0, 2, 4, ---, 18.

[Fig. 1.]

A typical picture of amplitude of the waves on (m, n-m) charts is shown in fig. 1 (May 500 mb). It is well known (Craham, (9); Van Isacker and Van Mieghem (25)) that the bulk of atmosphere's eddy energy is lodged in wave numbers one to eight. This is clearly brought out in Fig. 1, where the largest amplitude of 23.2 gpm was found for m=1, n-m=2. The amplitudes decreases to less than one-tenth of this value for $m \geq 5$ for all values of (n-m). We believe that when such normal charts become the reference charts for comparison with actual charts, prominent anomalies of actual charts would become perceptible and the persistance, growth or decay of such anomalies can be followed in course of time. May be, such anomalies will at some stage become a tool of long range forecasting.

We here present the analysis of normal charts for m = 1, 2 and (n-m) = 0 , 2 for the five months period March to July. Detailed analysis for other combinations of m and (n-m) will be presented elsewhere. Since

... 9

substantial part of eddy energy is concentrated in wave numbers 1 and 2 for (n-m) = 0 and 2, their discussion in a separate paper here is not in-appropriate. The discussion will also indicate the type and amount of information which is available in the analysis of normal charts.

Table 1 gives the amplitude of the wave and position of the ridge line at various isobaric levels, during different months. Greenwich meridian is reckoned as longitude of the phase zero. We shall briefly discuss important features of the four waves under study.

3.1 m = 1, n = 1 : [Fig. 2 (a), 2 (b)]

(Fig. 2 and Table 1), During March, the ridge line lies close to the longitudes of western Europe in the lower troposphere and over the longitudes of western Asia in the upper troposphere. In otherwords, the wave tilts eastward with increase of height. It transports heat southwards and tends to increase the intensity of north-south temperature gradient in the troposphere in the middle latitudes. During April to July, the wave moves further westward in the lower troposphere and remains nearly stationary in the upper troposphere, thus increasing the tilt in the vertical. During July, the ridge lies over western Atlantic in the lower troposphere and over the

.... 10

longitudes of east Iran, Afghanistan and western parts of Pakistan in the upper troposphere.

Amplitude of the wave is maximum around 200 mb level during March to May but increases upwards even at 100 mb level during June and July.

3.2 m = 1, n = 3 [Fig. 3 (a) and 3 (b)]

(Fig. 3 and Table 1), During March, the ridge lies close to the longitudes of west Asia in the lower troposphere and over eastern Atlantic in the upper troposphere. Thus the wave tilts westwards with height and transports heat northwards. From March to April, the wave moves westwards in the lower troposphere and slightly eastwards in the upper troposphere, with consequent decrease in the vertical tilt of the wave, even though the wave continues to tilt westward with height in the troposphere during the month of April also. This trend of movement continues from April to May. During the middle of May the wave axis is nearly vertical and lies along the longitudes of extreme west Europe. From May to June, the wave moves eastwards practically at all levels in the troposphere, movement being faster in the upper troposphere than in the lower troposphere. Consequently, the wave tilts eastward with height during June, transporting heat southwards. From June to

... 11

July, this eastward tilt with height gets further accentuated. By middle of July, the wave ridge is over western Atlantic in the lower troposphere and over the longitude of central China in the upper troposphere.

The amplitude of the wave is maximum around 200 mb level.

3.3 m = 2, n = 2 : [Fig. 4 (a), 4 (b)]

(Fig. 4 and Table 1), During March, the ridge lies over the longitudes of Afghanistan and Pakistan in the lower troposphere and over eastern Asia in the upper troposphere, with average eastward tilt with height. From March to April, the lower part of the wave moves eastwards while the upper part moves westwards, thus decreasing the eastward tilt of the wave. From April to May, the wave continues to move eastwards in the lower troposphere but remains practically stationary aloft. In this process, the tilt of the trough in the vertical gets reversed. By middle of May, the ridge lies over central Pacific in the lower troposphere and over the longitudes of central China in the upper troposphere, tilting westward with height. From May to July, the wave remains practically stationary.

... 12

The wave has maximum amplitude generally at 200 mb level.

3.4 m = 2, n = 4 [Fig. 5 (a), 5 (b)]

(Fig. 5 and Table 1), In middle of March, the wave ridge lies over the longitudes of western Asia in the lower troposphere and over the longitudes of east Mediterranean in the upper troposphere with westward tilt in the vertical. From March to May the wave moves slowly eastwards, the movement being a bit faster in the upper troposphere than in the lower troposphere. By middle of April, the wave axis is nearly vertical. It tilts slightly eastwards with height by middle of May. From May to July, the wave moves westward in the lower troposphere and eastward in the upper troposphere, considerably accentuating the eastward tilt of the wave. By middle of July, the ridge lies over the longitudes of central Sahara in the lower troposphere and over the longitudes of Burma in the upper troposphere.

From March to May, the maximum amplitude is at 300 mb level. During June and July, the amplitude is found to be increasing with height even upto 100 mb level.

4. Result of Fourier analysis at different latitudes :

Tables 2 (a to e) give the values of R_m and ϵ

... 13

(eq. 1a) for m = 1 and m = 2, for each of the five months March to July, at different isobaric levels and at different latitude circles. The phase refers to ridge line. From the orientation of the ridge line at an isobaric level, we can get qualitative idea of north-south transfer of westerly momentum Starr, (23). The transfer of westerly momentum is northward if the orientation of the ridge line is in a NE - SW direction and the transfer is southward if the orientation is in a NW - SE direction. From the vertical tilt, we can as before infer the eddy transport of sensible heat.

It is uninteresting to describe in detail the variation seen in different tables given above. The detailed variations in space and time are not very smooth. Nevertheless, there is a definite pattern seen in each table and we can trust the large scale feature seen in these tables. Some of these features are described below.

4.1 : Vertical tilt.

m = 1. /Fig. 6 (a)/

At 20°N and 30°N, the ridge line tilts eastward with height upto and below 300 mb level in all the months.

... 14

At 40°N, during March and April, the tilts are variable; but during May, June and July the ridge tilts eastward with height. At 50°N, the tilt is westward and feeble during March and April, is slightly eastward during May and becomes progressively more easterly during June and July. At 60°N, the tilt is westerly during March, decreases in intensity but remains westerly during April and becomes a weak easterly tilt during May and June. The tilt becomes westerly during July.

m = 2. [Fig. 6 (b)]

At 20°N, from March to July, the ridge tilts generally westward with height. Therefore, it transports heat northwards from the tropics.

At 30°N, the tilts are very weak in the lower troposphere during all the months. In the middle and upper troposphere, the ridge tilts westward with height.

At 40°N, the tilt is weak westerly during March and weak easterly during April. From May to June, the eastward tilt is more pronounced particularly in the lower troposphere. During July, the tilt is westward.

At 50°N, the picture is more regular. The tilt is westerly during March, weak westerly during April;

practically vertical during May; slightly easterly during June and more easterly during July.

At 60°N, the picture is equally regular. The tilt is westerly during March, decreases but remains westerly during April, is nearly vertical during May and easterly during June and July.

4.2 Horizontal tilt :

It is observed that the horizontal tilts of the wave are generally weak between the latitudes 15°N and 30°N and also between the latitudes 45°N and 60°N for both wave numbers 1 and 2. There are also abrupt displacements in the ridge positions between 30°N and 45°N. This appears to be due to the position of the eastwest running subtropical ridge in the lower troposphere which separates westerlies and easterlies on its two sides and in the vicinity of which north-south running trough and ridges are not well marked. Similar abrupt displacements also occur in the polar latitudes near the region of the east-west running polar front.

Other important features of horizontal tilt for m = 1, 2 are discussed below.

m = 1.

... 16

[Fig. 7 (a)]

850 mb : The ridge tilts westward in the lower latitudes in all the months. In the middle latitudes, the tilt is eastward. From 60°N to 80°N, the ridge tilts generally westward.

700 mb : In the lower latitudes, the wave tilts eastward during March and April but has nearly north-south orientation from May to July. The tilt is generally eastward from 30°N to 50°N and westward from 60°N to 80°N.

500 mb : The tilt is westward in the lower latitudes. In the middle latitudes, the tilt is weak during March to May, but eastward during June and July. The amplitude and phase obtained here generally compare well with the values obtained by Eliasen (5) for July normal height data, though there are differences in amplitude at 50°N. The months of March and April form the pattern distinct from other months. Van Mieghem (26) found eastward meridional tilt of the long stationary wave for Jan. - April 1953 at 50°N but, in our results the tilts are weak and indifferent.

300 mb : The ridge line tilts eastward in the lower latitudes. In the middle latitudes, tilts are weak from March to May but eastward during June and July.

... 17

200 mb : March and April form a pattern in which the ridge orientation is practically north-south from 10°N to 30°N. The tilt is westward from 30°N to 45°N, and again eastward north of 70°N. During June and July, the tilt is found to be eastward between 10°N and 30°N and again between 40°N and 55°N. This also agrees with the findings of Krishnamurty (14) who analysed 200 mb flow pattern during the summer months of 1967.

100 mb : The orientations are qualitatively similar to those at 200 mb level.

m = 2.

[Fig. 7 (b)]

850 and 700 mb : Except in the regions of subtropical ridge line and the polar front, the tilts are generally westward.

500 mb : The tilts are similar to those at 850 mb and 700 mb levels except that during the month of July at 500 mb level, the ridge tilts eastward from equator to 20°N.

300 mb : North of 10°N, the tilts are generally westward.

200 mb : The tilts are generally westward except that

.../. 18

during July, the ridge line tilts towards east from 15°N to 50°N.

100 mb : During March and April, the tilts are westward from 5° to 50°N. The tilts are very weak between 50°N and 60°N. May acts as a transitional month with an easterly tilt from equator to 30°N. During June, the tilts are easterly from equator to 30°N and very weak from 30°N to 70°N. During July, the tilt is easterly at all latitudes, the tilts being strong south of 20°N and north of 65°N.

5. Conclusions :

(i) We believe that large scale anomalies in the behaviour of the Indian summer monsoon are dynamically related to the anomalies in the global flow pattern with periods larger than the summer season. Hence it may be possible, in course of time, to predict anomalies of Indian summer monsoon with the help of anomalies of the global flow pattern observed a couple of months in advance. A first step in this direction is to have global normal charts for variaous levels so that one can work the departures of observed pattern from the normal patterns. Due to difficulties of data in the southern hemisphere, we have for the time being confined ourselves to the northern hemisphere. It is however, not suggested

... 19

that southern hemisphere has no significant part to play.

(ii) Normal upper air charts of the northern hemisphere prepared by the Free University of Berlin, have been subjected to spherical harmonic analysis for $m = 0, 1, 2, \ldots, 18$ and $n-m = 0, 2, 4, 6, \ldots, 18$. In this paper, we have presented somewhat detailed analysis for $m = 1, 2$ and $n-m = 0, 2$ for the months March to July. The vertical and the horizontal tilts of the waves are discussed. Climatological information of this type will serve as a good reference material for study of the anomalies of geopotential pattern in any particular year.

Acknowledgement :

We took help from Shri H.S. Bedi and Shri G. Appa Rao in computer programming. The authors have greatly benefited from discussions with Shri S.K. Mishra. Shri H.P. Das, Shrimati Leela George, Shri J.M. Pathan and Shri M.B. Gajare considerably helped in collection and processing of the data. We acknowledge our sincere thanks to all of them.

REFERENCES

1. Baer, F., and Platzman G.W. — A procedure for numerical integration of the spectral vorticity equation. J.Met., 18, 393-401 (1961).

2. Baer, F. — Integration with the spectral vorticity equation. J.Atmos. Sc. 21, 260-276 (1964).

3. Blinova, E.N., — Hydrodynamical theory of pressure and temperature waves and of centres of action. C.R. Acad. Sc. U.R.S.S. 39, 257.

4. Craig, R.A. — A solution of the non linear vorticity equation for atmospheric motion. J.Met., 2, 173-178, (1945).

5. Eliasen, E. — A study of the long atmospheric waves on the basis of zonal harmonic analysis. Tellus, 10, 206-216 (1958).

6. Elissen, E. and Machenhauer, B. — On the observed large scale atmospheric wave motion. Tellus, 21, 149-166 (1969).

7. Ellsaasser, H.W. — Expansion of hemispheric meteorological data in antisymmetric surface spherical harmonic (Laplace) series. J.Applied Met. 5, 263-276, (1966).

8. Free University of Berlin, Berlin. — Institute of Meteorology and Geophysics, Free University of Berlin, Berlin, 100, No. 1 (1969).

... 2

9. Graham, R.D. — An empirical study of planetary waves by means of harmonic analysis. J.Met. 12, 298-307 (1955).

10. Haurwitz, B. — The motion of atmospheric disturbance on the sperical earth. J.Marine Res.3, 254-267, (1940).

11. Haurwitz, B. and Craig, R.A. — Atmospheric Flow patterns and their representation by spherical surface Harmonics, Geophy. Res. Paper No. 14, 3-78 (1952).

12. Jagannathan, P. — Seasonal forecasting in India. A Review. (India Met. Dep. Publication) (1960).

13. Keshavamurty, R.N. and Awade, S.T. — Dynamical abnormalities associated with drought in the Asiatic summer monsoon. International Tropical Sym., Nairobi (Kenya), Feb. (1974).

14. Krishnamurty, T.N. — Observational study of the tropical upper tropospheric motion field during the northern hemispheric summer. J.Applied Met. 10, 1066-1096, (1971).

15. Kubota, S. — Surface spherical harmonic representation of the system of equations for analysis. Paper in Meteor. Geophys (Tokyo). 10, 145-160, (1960).

... 3

16. Merilees, P.E. — The equations of motion in spectral form. J.Atmos.Sc.25,736-743 (1968).

17. Neamtan, S.M. — The motion of Harmonic waves in the atmosphere. J.Met. 3, 53-56 (1946).

18. Platzman, G.W. — The spectral form of the vorticity equation. J.Met. 17, 635-644 (1960).

19. Raghavendra, V.K. and Robert, R.W. — Seasonal forecasting in India Vayu Mandal, 3, 84-90 (1973).

20. Rao, K.N. — Seasonal forecasting India. W.M.O. Technical Note No. 66. 1726 (1964).

21. Saltzman, B. — Steady state solution for the axially symmetric climate variable. Pure Appl. Geophys. 69, 237-259 (1968).

22. Silberman, I. — Planetary waves in the atmosphere. J.Met. 11, 27-34 (1954).

23. Starr, V.P. — An essay on the general circulation of the earth's atmosphere. J.Met. 5, 39-43 (1948).

... 4

24. Walker, G.T. — Memorandum on the meteorological conditions prevailing in the India monsoon region during the first half of the southwest monsoon period of 1906 with anticipations regarding the monsoon rainfall during August and September 1906. — India Met. Dep. Mem. XII part IV, 1-9, (1906).

25. Van Isacker and Van Mieghem — De selective rol Van de atmosferische storingen in de algemene luchtcierculatie Med. Kon. Vlaamse Acad. Van Belgie, K.I. 18, 3-18 (1956).

26. Van Mieghem — " On the selective role of the motion systems in the atmospheric general circulation ".

The atmosphere and the sea in motion. The-Rossby memorial volume., 230-238, (1959).

...

TABLE - 1

Amplitude (gpm) of the waves and phase of the ridge lines

MONTH			MARCH		APRIL		MAY		JUNE		JULY	
m.	n	MB	Amp	Phase	Amp	Phase	Amp	Phase	Amp	Phase	Amp	Phase
1	1	850	2.8	2	7.0	319	15.3	301	24.4	290	31.8	276
1	1	700	7.6	15	11.9	1	15.4	336	20.8	316	26.1	292
1	1	500	14.9	1	16.5	20	20.6	7	14.4	350	13.9	310
1	1	300	15.6	42	17.5	61	34.5	49	32.3	35	27.1	47
1	1	200	21.2	47	33.1	54	30.4	54	43.3	67	55.7	66
1	1	100	19.7	43	18.4	74	26.7	45	58.6	63	70.3	64
1	3	850	7.5	51	12.7	19	13.0	351	10.3	324	9.4	288
1	3	700	13.5	27	18.9	11	14.4	355	8.3	3	3.9	296
1	3	500	28.0	345	26.6	357	23.2	358	11.9	29	6.0	77
1	3	300	31.1	345	22.5	354	19.7	16	8.6	57	25.6	104
1	3	200	40.6	329	36.5	347	17.1	338	18.2	42	37.0	105
1	3	100	26.7	301	11.4	299	14.6	106	12.9	52	35.8	113
2	2	850	1.6	76	3.7	158	10.6	166	16.3	165	19.5	163
2	2	700	3.9	61	2.8	78	5.2	177	10.0	172	13.8	160
2	2	500	4.3	59	8.3	85	4.4	108	0.4	180	7.7	144
2	2	300	3.6	175	15.9	105	17.2	106	12.3	102	14.7	105
2	2	200	10.2	127	28.4	108	25.9	106	25.2	97	27.2	92
2	2	100	6.3	120	17.0	112	19.6	97	33.7	86	24.7	86
2	4	850	15.0	57	11.6	66	10.4	56	8.3	33	9.4	11
2	4	700	17.9	48	15.5	60	14.0	60	11.3	54	4.4	46
2	4	500	27.0	34	22.8	54	21.0	66	15.3	72	16.8	76
2	4	300	41.9	28	20.5	52	19.5	69	17.6	82	18.7	94
2	4	200	35.1	29	21.4	57	16.8	75	26.5	81	29.2	97
2	4	100	27.3	22	20.0	50	13.2	57	34.1	86	37.7	93

TABLE 2 (a)

Amplitude (gpm) and phase of ridge lines (Harmonic Analysis)

MARCH

	LAT	Eq		20°N		30°N		40°N		50°N		60°N		80°N	
	MB	R_m	ϵ	R_m	ϵ	R_m	ϵ	R_m	ϵ	R_m	ϵ	R_m	ϵ	R_m	ϵ
m=1	850	0.7	93	0.4	287	16.1	260	7.0	18	32.8	50	20.2	46	27.7	184
	700	8.2	281	4.2	334	8.7	247	17.7	14	37.8	32	38.3	12	19.2	161
	500	2.8	169	8.5	82	14.2	266	38.1	344	65.4	356	70.1	353	11.6	160
	300	5.5	84	27.8	94	22.7	166	15.2	293	80.6	357	99.6	354	29.5	88
	200	26.2	102	38.4	94	23.7	77	33.7	347	76.2	336	95.4	339	31.3	52
	100	8.6	35	43.8	82	39.4	84	24.7	21	48.4	303	84.3	312	11.3	198
m=2	850	0.2	152	14.1	143	7.4	176	21.9	57	43.8	64	24.9	60	11.7	1
	700	1.8	104	11.8	124	1.6	15	28.8	58	45.6	53	35.9	37	20.4	358
	500	1.2	136	22.7	110	8.9	139	40.6	41	37.1	39	54.0	26	42.4	10
	300	0.7	29	38.7	117	23.8	134	63.9	28	97.2	34	90.4	23	43.1	16
	200	8.0	147	48.7	120	49.1	111	32.3	37	88.1	26	100.6	20	45.1	19
	100	2.4	74	40.1	116	36.2	111	20.4	46	63.0	19	105.5	14	53.1	20

TABLE 2 (b)

Amplitude (gpm) and phase of ridge lines (Harmonic Analysis)

APRIL

		Eq		20°N		30°N		40°N		50°N		60°N		80°N	
	MB	R_m	ϵ	R_m	ϵ	R_m	ϵ	R_m	ϵ	R_m	ϵ	R_m	ϵ	R_m	ϵ
m=1	850	4.4	348	12.1	241	19.9	246	16.5	349	40.7	18	30.8	22	13.2	235
	700	1.2	251	2.6	344	9.1	276	28.4	358	57.6	12	41.1	18	9.8	215
	500	0.0	178	10.9	66	6.8	105	26.1	352	81.6	355	67.4	7	13.2	183
	300	9.6	106	29.2	91	30.9	164	12.1	205	75.6	9	88.1	6	17.9	136
	200	17.6	104	42.1	91	41.3	112	59.8	13	92.4	355	82.8	359	10.9	109
	100	3.9	22	44.4	91	40.1	131	29.4	125	31.5	352	51.1	323	13.2	273
m=2	850	2.5	172	14.8	163	16.3	158	8.2	80	34.8	66	32.9	66	12.4	7
	700	1.7	163	6.8	125	9.8	157	19.3	78	42.6	61	40.0	52	15.6	31
	500	0.0	88	16.9	117	19.5	110	28.9	77	64.6	51	52.5	46	17.4	18
	300	3.8	37	45.1	114	38.0	120	22.1	93	76.8	54	65.8	39	26.1	13
	200	18.7	120	45.1	111	50.5	123	57.2	90	58.7	58	52.0	38	32.7	11
	100	7.6	4	45.6	114	37.4	104	22.6	78	43.5	47	40.8	33	10.8	25

TABLE 2 (c)

Amplitude (R_m) and phase of ridge lines (Harmonic Analysis)

MAY

		Eq		20°N		30°N		40°N		50°N		60°N		80°N	
		R_m	ϵ	R_m	ϵ	R_m	ϵ	R_m	ϵ	R_m	ϵ	R_m	ϵ	R_m	ϵ
m=1	850	9.4	341	18.7	200	34.0	279	26.4	332	40.0	359	25.6	347	12.4	217
	700	5.3	300	18.7	335	21.3	286	29.3	348	47.3	6	34.7	351	18.1	205
	500	2.1	134	20.2	12	13.7	319	43.8	357	75.1	8	44.3	3	10.5	159
	300	3.7	19	45.1	60	44.6	108	46.8	25	85.7	16	60.7	18	40.1	135
	200	3.8	340	63.4	74	49.4	113	21.3	339	67.3	357	52.7	6	44.6	105
	100	69.0	312	59.6	74	55.1	99	14.1	74	27.7	15	33.3	38	50.2	83
m=2	850	6.0	176	23.8	161	29.2	168	7.4	50	29.5	61	23.9	58	6.1	11
	700	1.9	142	21.0	167	14.1	172	13.8	69	38.1	63	30.1	53	7.3	3
	500	1.9	163	12.6	152	12.5	131	39.2	81	57.2	67	39.9	49	14.3	174
	300	3.1	108	29.8	119	35.7	117	49.2	95	55.6	65	49.6	46	25.0	9
	200	4.1	147	46.8	107	68.1	119	37.0	98	53.6	66	48.0	50	15.9	16
	100	14.8	12	40.7	99	58.1	110	29.2	96	28.7	69	32.3	50	7.7	85

TABLE 2 (d)

Amplitude (gpm) and phase of ridge lines (Harmonic Analysis)

JUNE

		Eq		20°N		30°N		40°N		50°N		60°N		80°N	
	MB	R_m	ϵ	R_m	ϵ	R_m	ϵ	R_m	ϵ	R_m	ϵ	R_m	ϵ	R_m	ϵ
m=1	850	10.0	16	36.3	271	52.6	284	39.3	304	27.6	338	7.6	333	31.3	288
	700	3.6	319	28.3	310	40.0	290	40.4	324	34.4	9	18.3	68	23.1	283
	500	1.7	43	14.7	338	22.3	302	48.0	337	46.8	28	32.8	82	17.4	254
	300	1.5	316	47.5	36	33.3	50	58.0	350	60.2	44	70.4	83	6.1	70
	200	17.2	151	69.6	73	69.0	76	39.9	14	52.2	38	74.1	68	30.9	102
	100	8.9	80	99.5	66	98.3	68	65.1	52	59.9	48	42.5	61	34.2	93
m=2	850	2.1	177	35.6	159	40.0	163	10.6	4	21.9	44	27.2	41	10.7	40
	700	1.3	94	29.4	164	23.6	172	8.0	63	31.3	60	29.9	49	9.2	44
	500	4.4	176	20.2	169	7.2	145	33.2	83	42.0	66	21.4	57	5.5	22
	300	3.3	79	11.5	131	23.8	107	44.1	94	37.8	85	31.1	58	5.1	34
	200	5.8	172	33.3	93	53.4	100	67.1	99	41.1	94	45.4	66	6.9	28
	100	5.7	35	33.0	84	75.2	91	80.0	88	31.2	80	43.9	80	7.5	180

TABLE 2 (e)

Amplitude (gpm) and phase of ridge lines (Harmonic Analysis)

JULY

		Eq		20°N		30°N		40°N		50°N		60°N		80°N	
	MB	R_m	ϵ	R_m	ϵ	R_m	ϵ	R_m	ϵ	R_m	ϵ	R_m	ϵ	R_m	ϵ
m=1	850	12.8	17	45.5	269	68.6	269	57.1	287	29.8	294	9.4	201	24.6	333
	700	10.1	301	34.6	293	49.3	285	53.3	300	23.4	301	18.2	151	7.7	45
	500	0.4	79	26.9	312	32.2	313	28.6	310	13.0	351	35.8	116	21.4	98
	300	9.9	272	46.3	23	62.7	43	34.8	6	30.9	105	81.2	116	63.7	89
	200	10.9	303	77.2	55	131.2	64	66.7	58	57.2	111	99.1	111	78.9	92
	100	19.5	38	77.6	47	128.1	66	130.9	76	67.8	100	59.7	119	34.7	88
m=2	850	2.2	4	35.9	157	45.9	161	24.1	170	23.6	25	23.3	37	13.2	85
	700	4.1	175	31.2	159	31.4	156	5.3	142	14.6	44	25.3	49	0.7	42
	500	2.9	141	22.3	160	18.0	146	19.3	110	15.0	57	20.6	55	1.4	52
	300	7.3	7	8.2	135	41.3	103	58.9	101	23.9	104	20.7	51	12.1	48
	200	10.0	141	21.3	83	71.0	88	90.1	98	40.4	113	19.7	75	5.3	59
	100	10.7	1	27.0	76	68.8	87	90.6	91	43.1	93	27.6	99	2.7	149

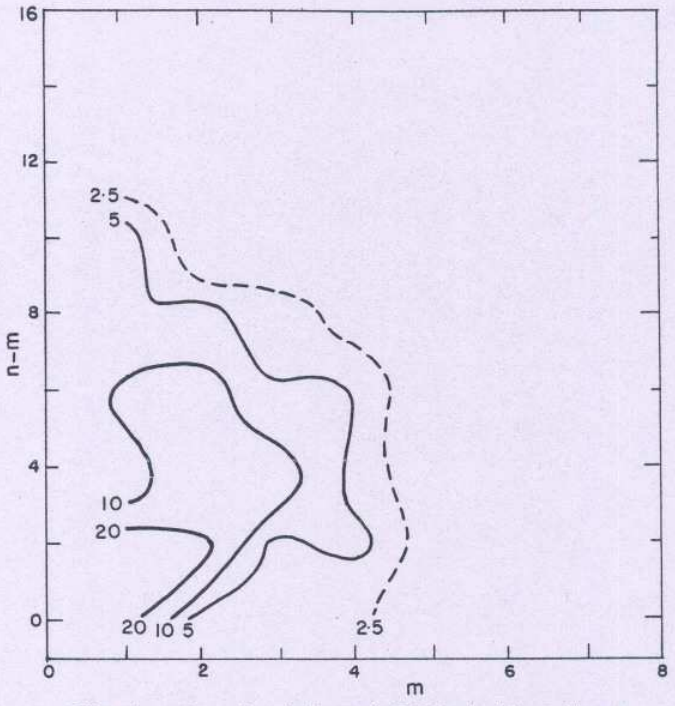

Fig. 1 Amplitude (gpm), 500 mb, May-Mean Height Data.

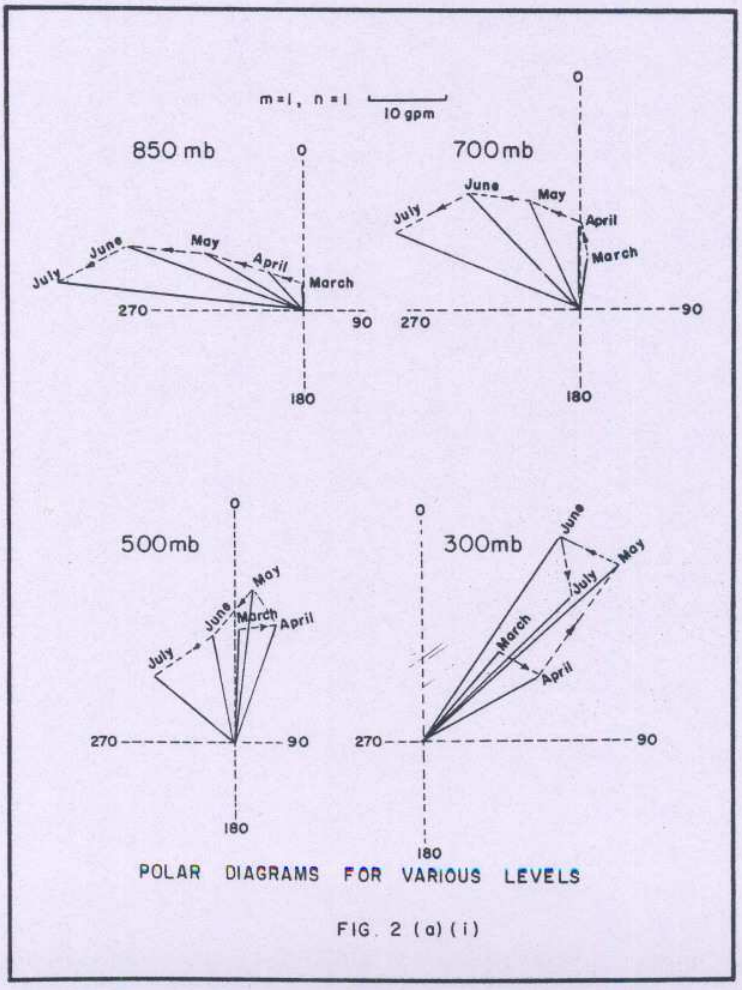

POLAR DIAGRAMS FOR VARIOUS LEVELS

FIG. 2 (a) (i)

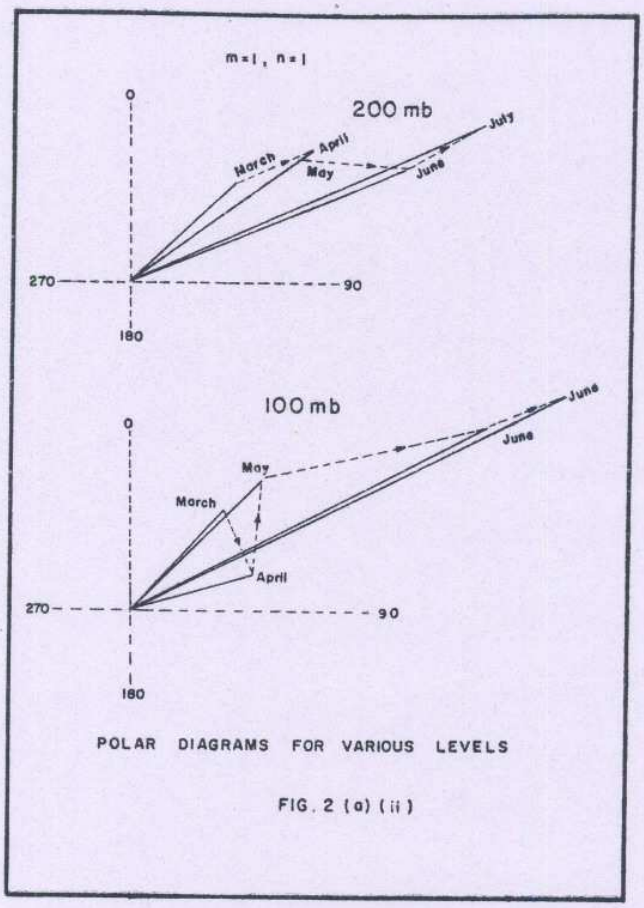

POLAR DIAGRAMS FOR VARIOUS LEVELS

FIG. 2 (a) (ii)

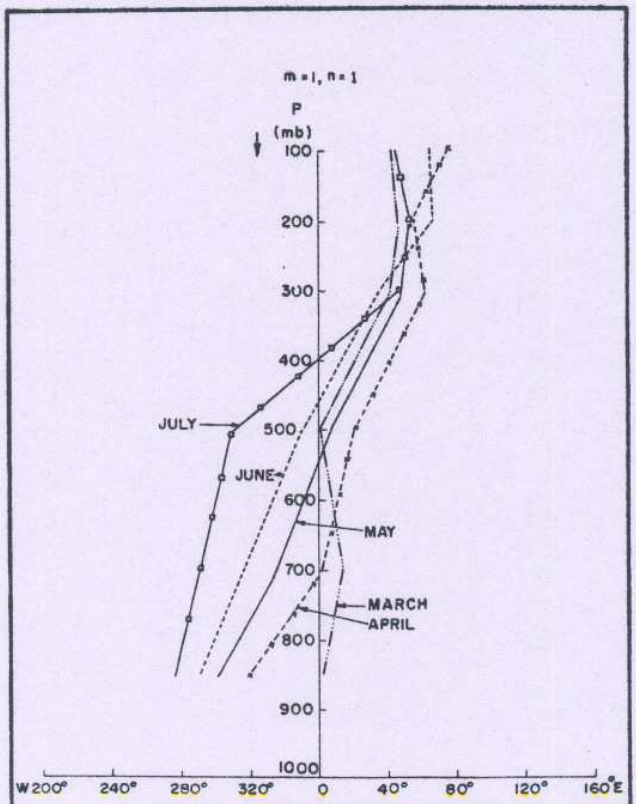

PHASE IN LONGITUDE(RIDGE LINE)

FIG. 2 (b)

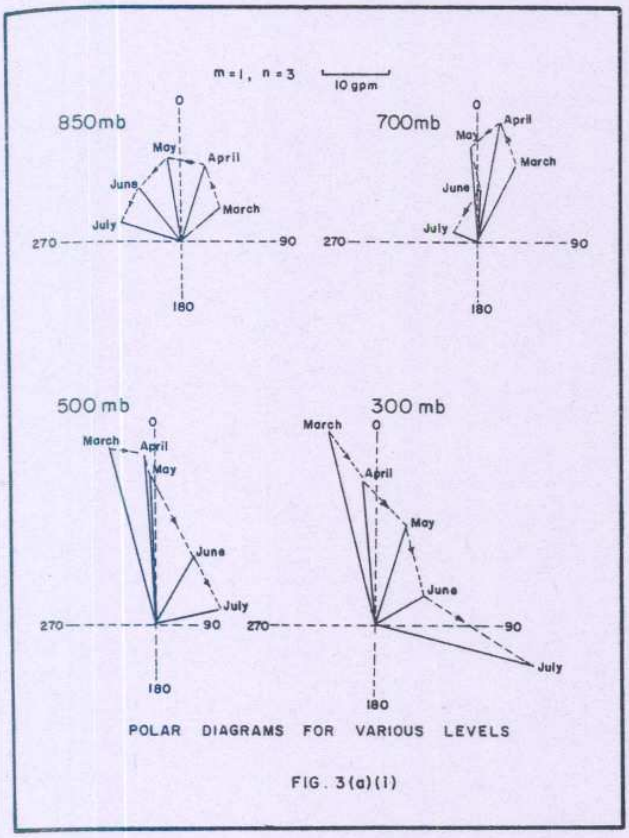

POLAR DIAGRAMS FOR VARIOUS LEVELS

FIG. 3(a)(i)

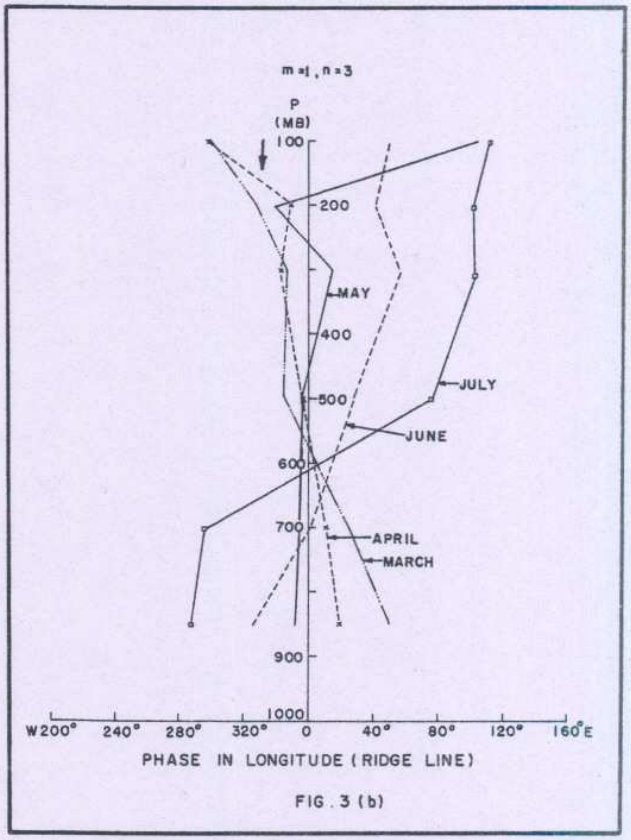

PHASE IN LONGITUDE (RIDGE LINE)

FIG. 3 (b)

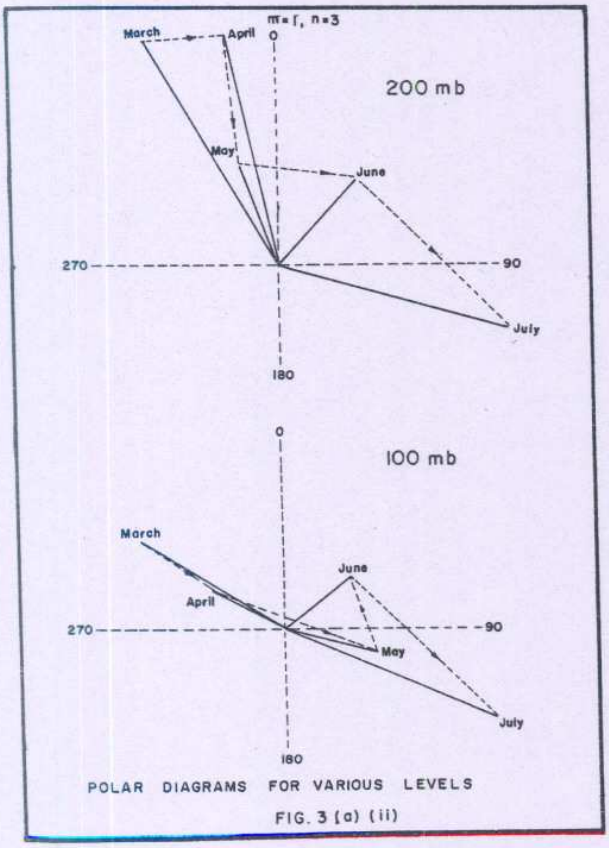

POLAR DIAGRAMS FOR VARIOUS LEVELS

FIG. 3 (a) (ii)

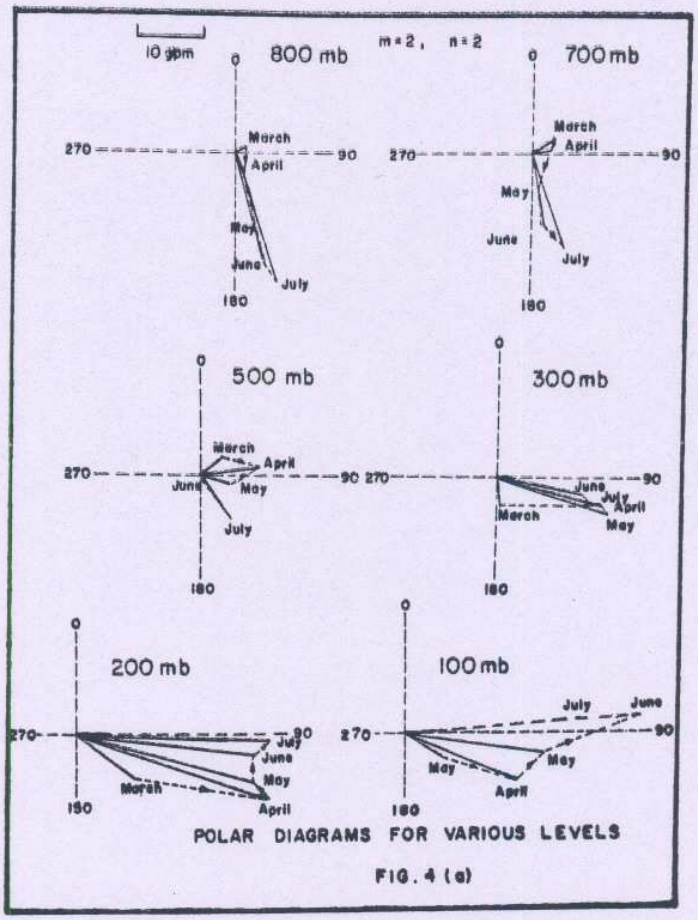

POLAR DIAGRAMS FOR VARIOUS LEVELS

FIG. 4 (a)

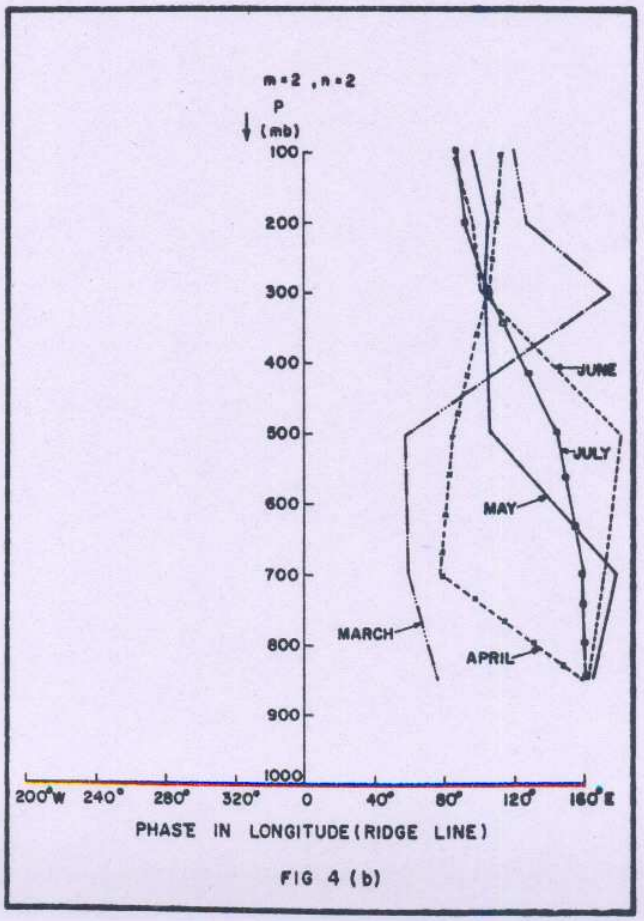

PHASE IN LONGITUDE (RIDGE LINE)

FIG 4 (b)

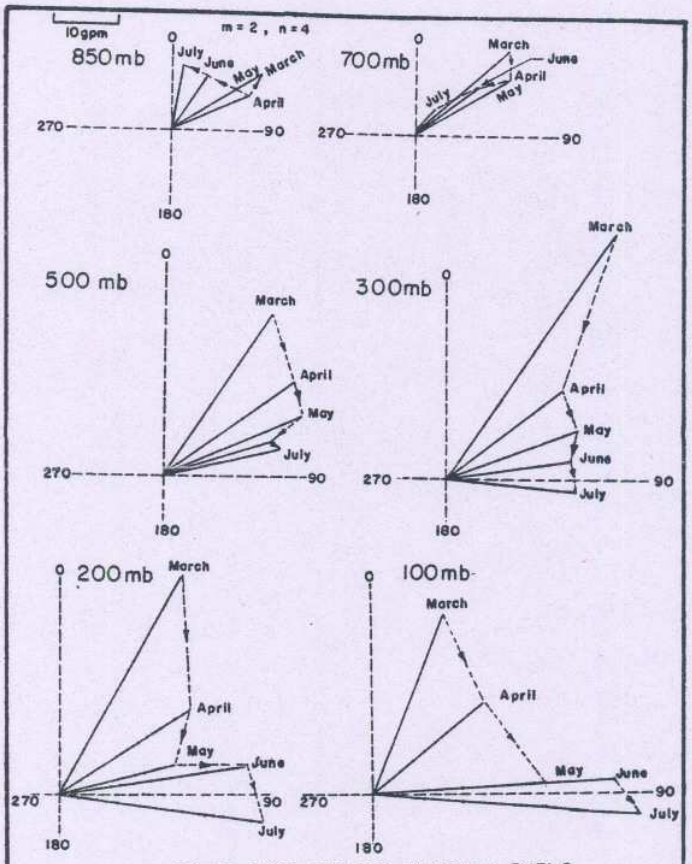

POLAR DIAGRAMS FOR VARIOUS LEVELS

FIG. 5 (a)

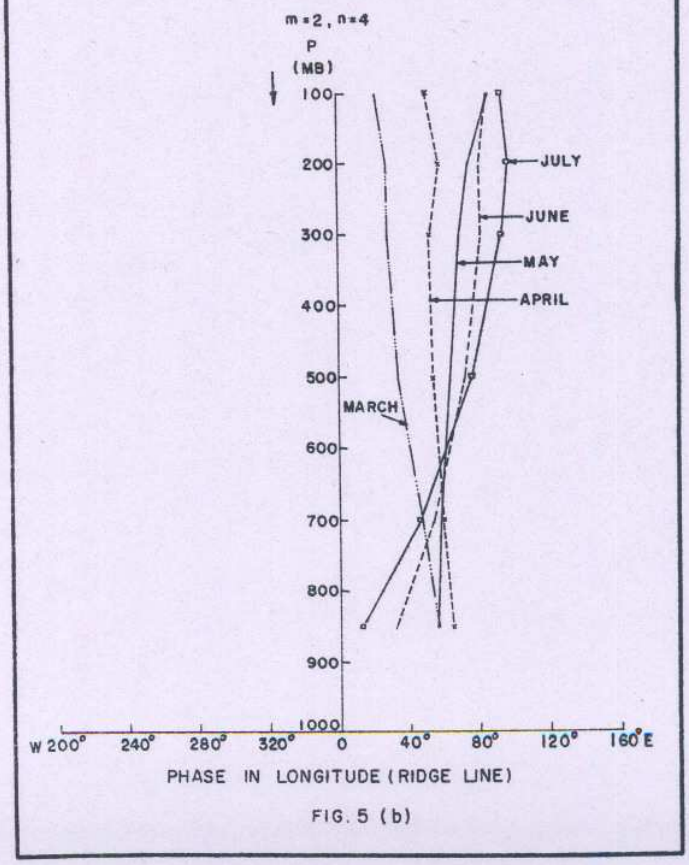

PHASE IN LONGITUDE (RIDGE LINE)

FIG. 5 (b)

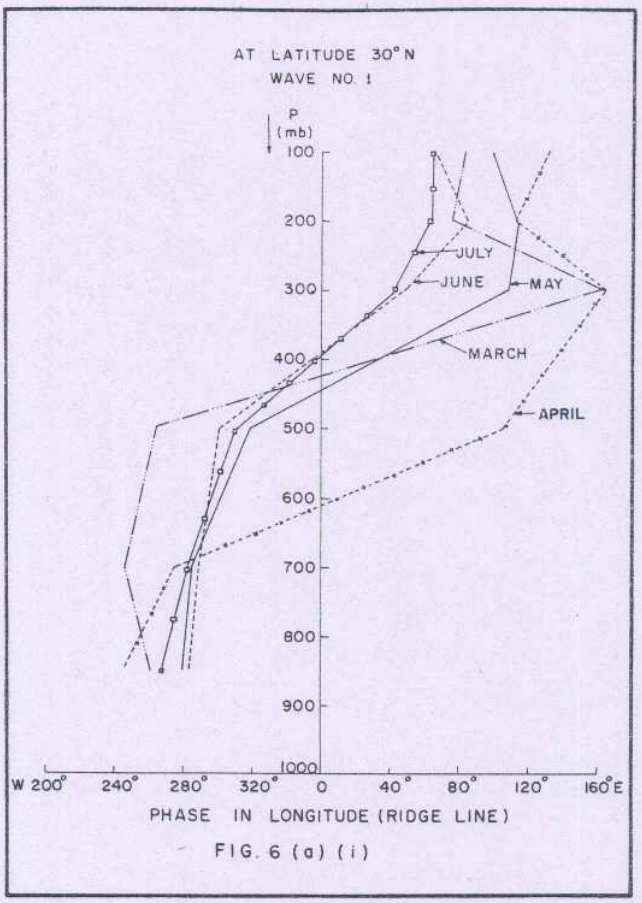

FIG. 6 (a) (i)

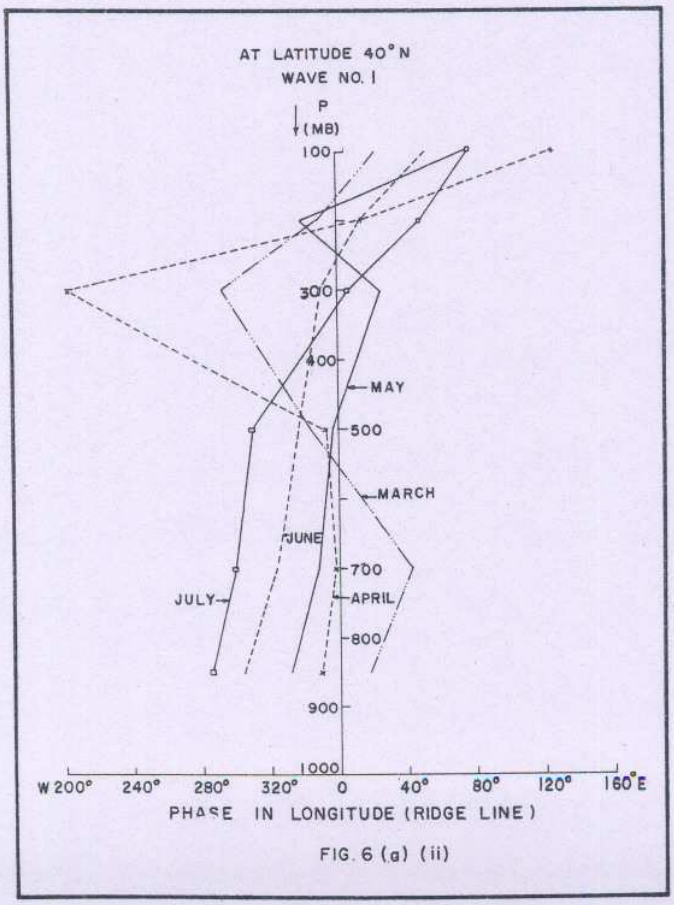

FIG. 6 (a) (ii)

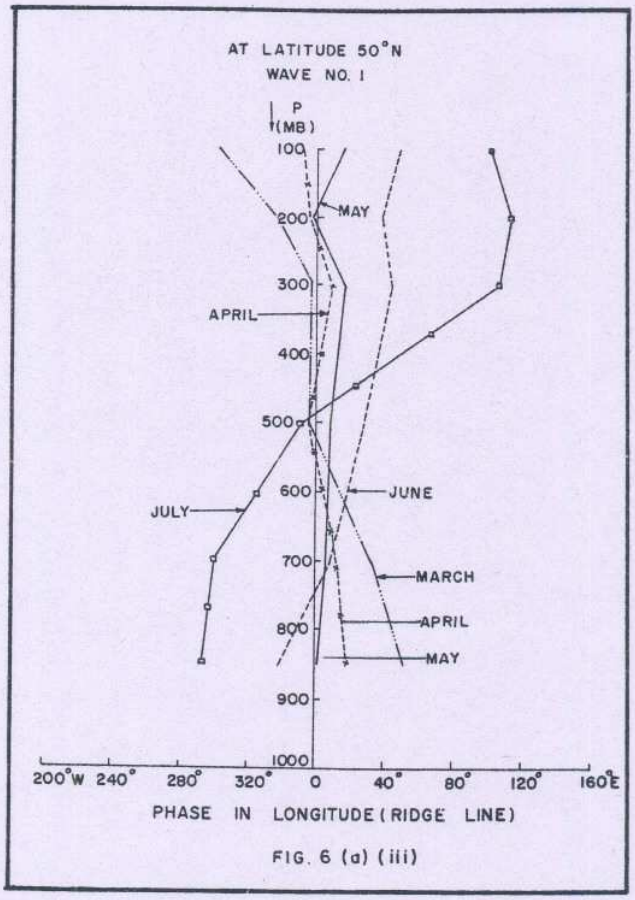

FIG. 6 (a) (iii)

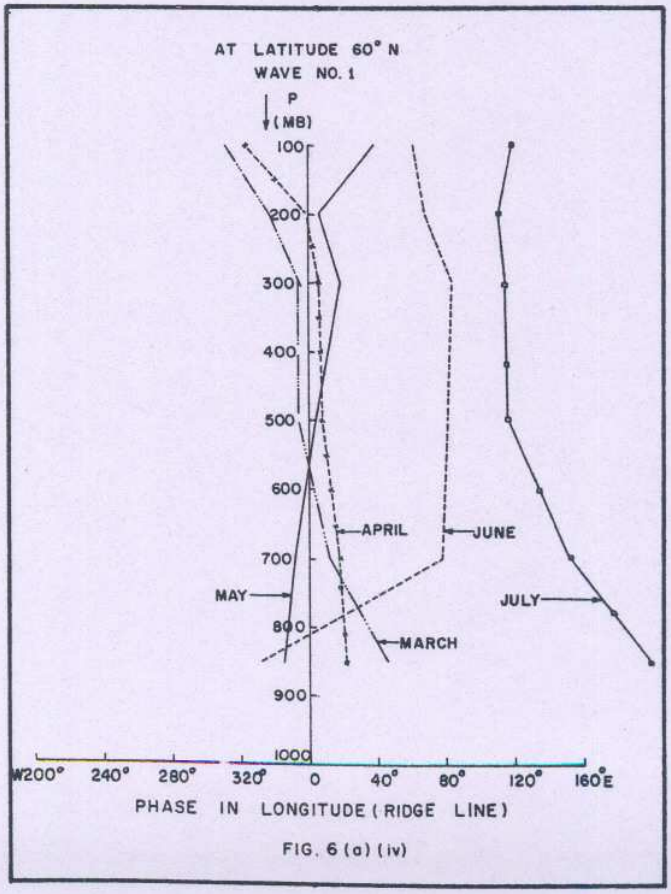

FIG. 6 (a) (iv)

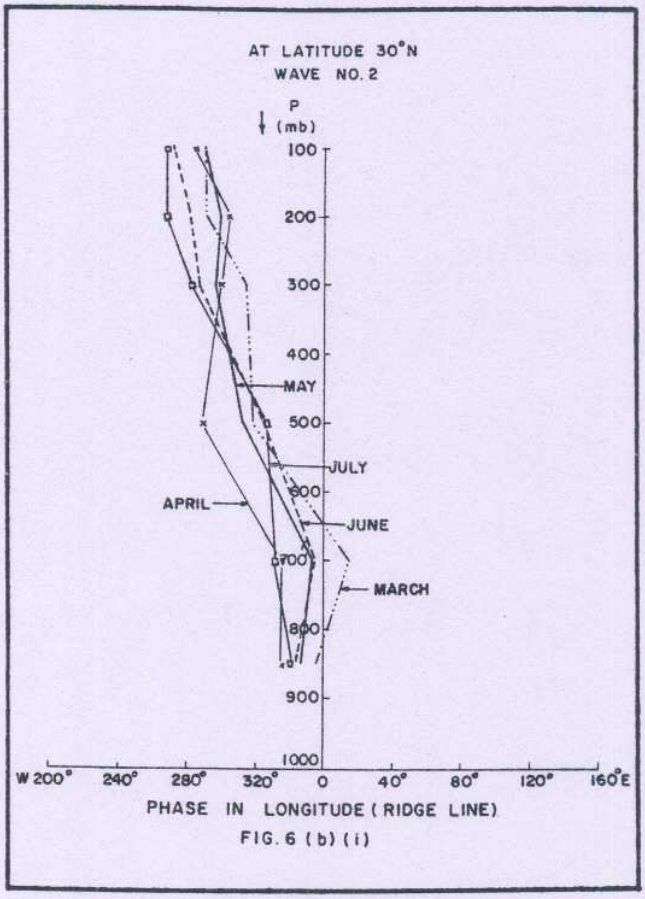

FIG. 6 (b) (i)

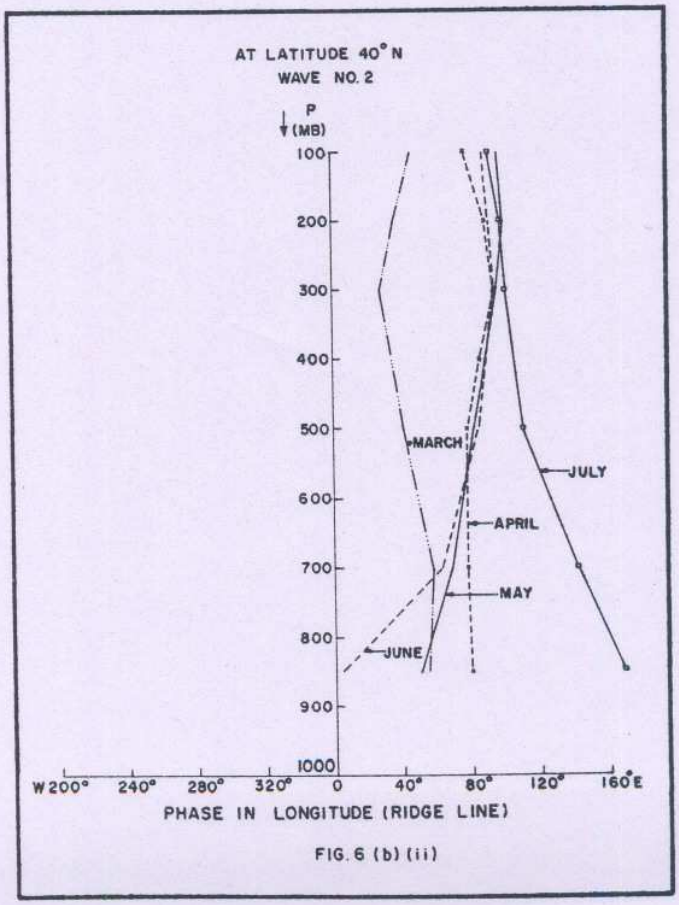

FIG. 6 (b) (ii)

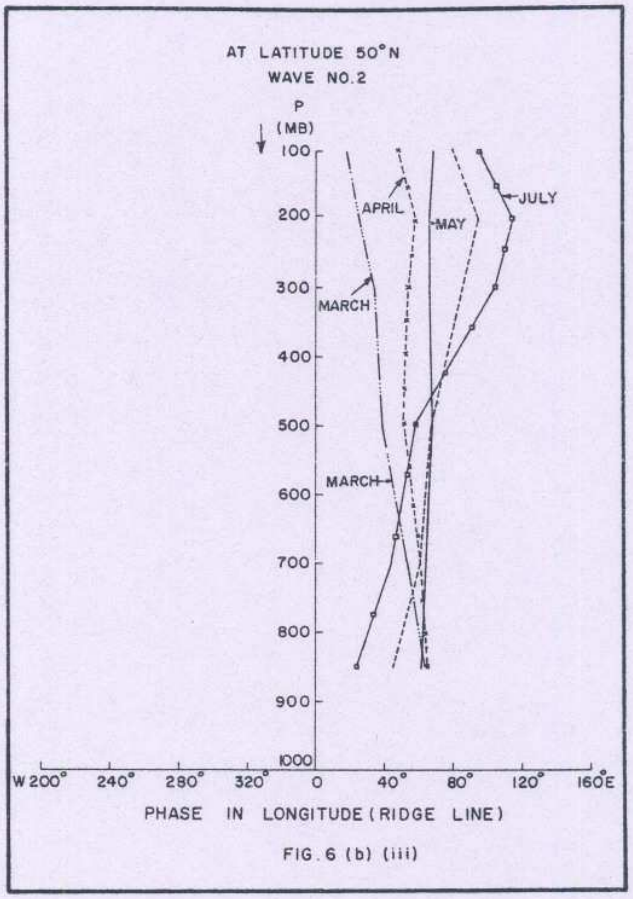

FIG. 6 (b) (iii)

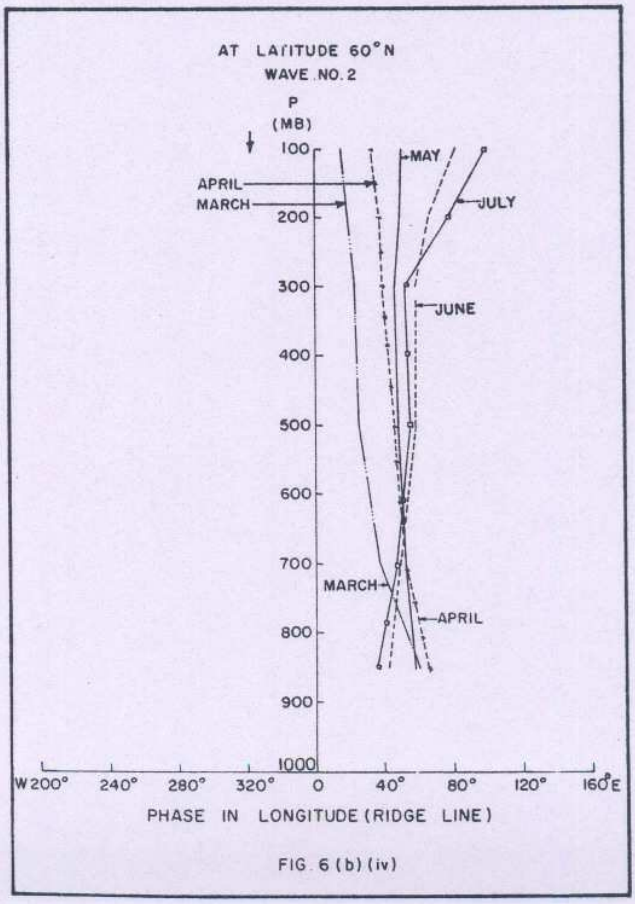

FIG. 6 (b) (iv)

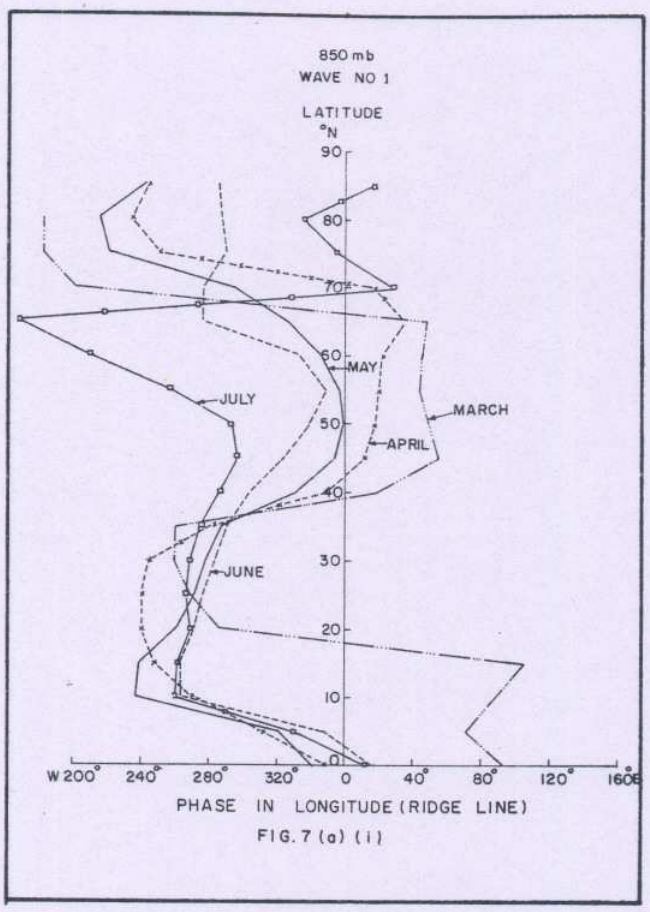

FIG. 7 (a) (i)

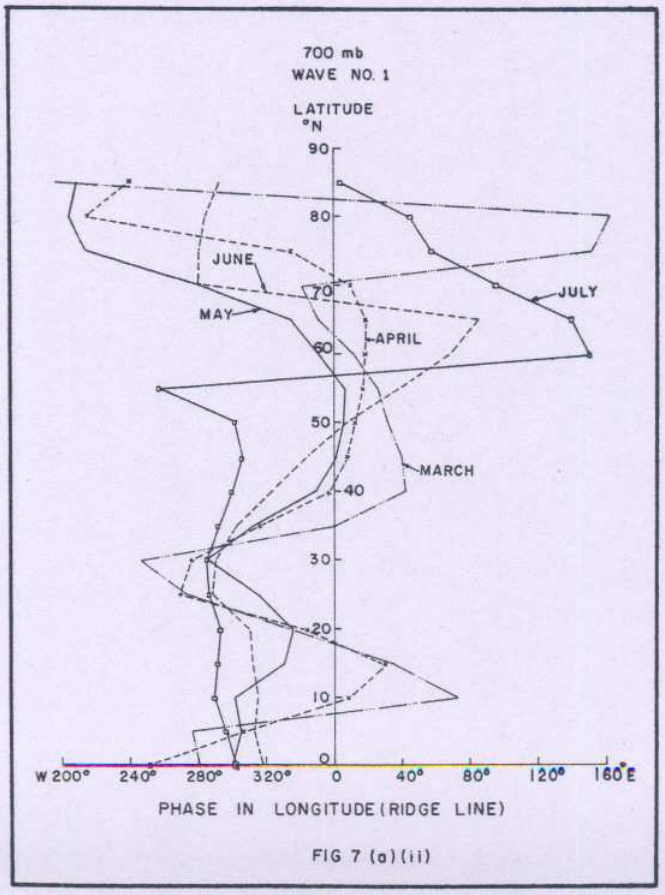

FIG 7 (a) (ii)

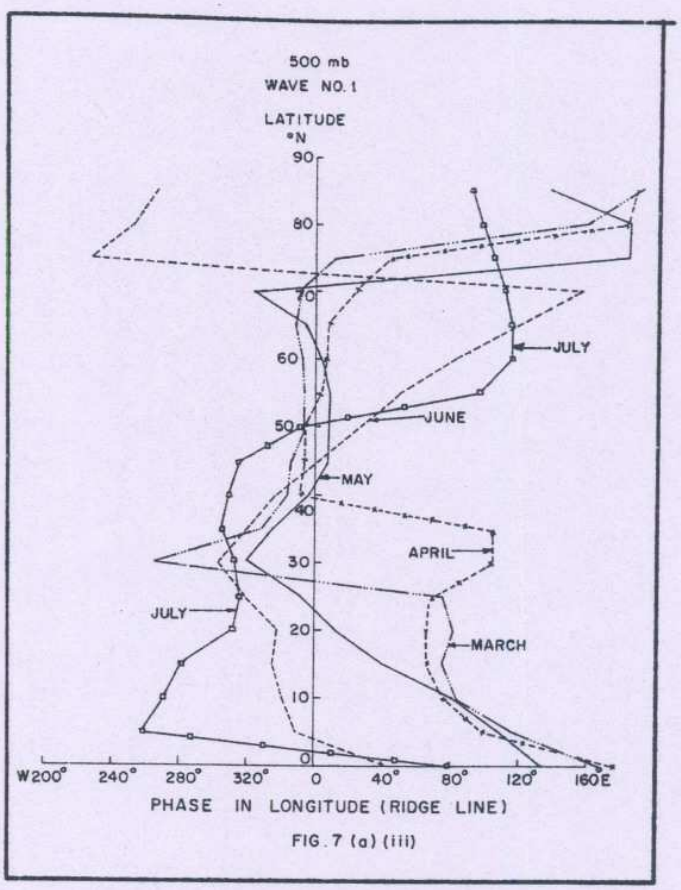

FIG. 7 (a) (iii)

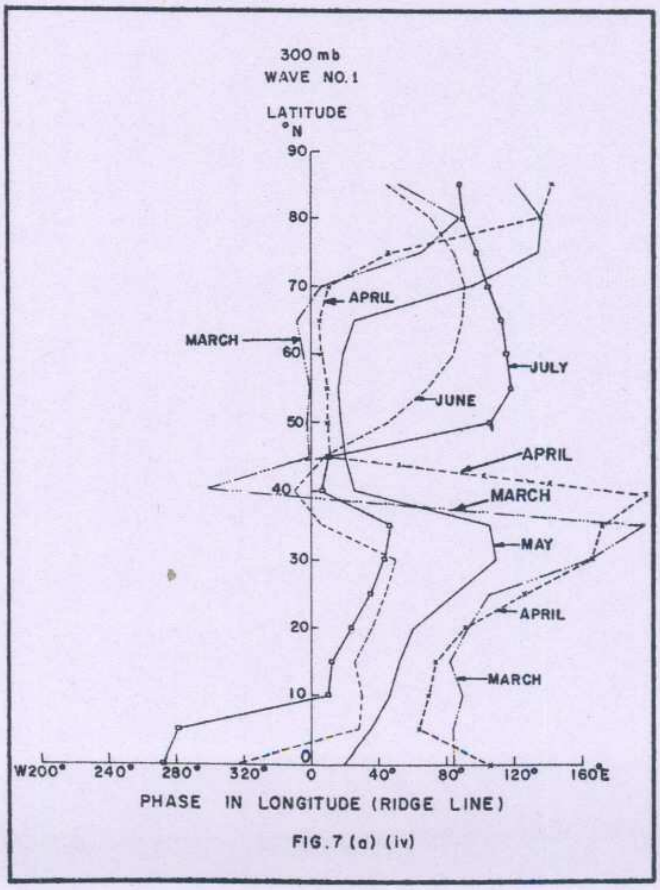

FIG. 7 (a) (iv)

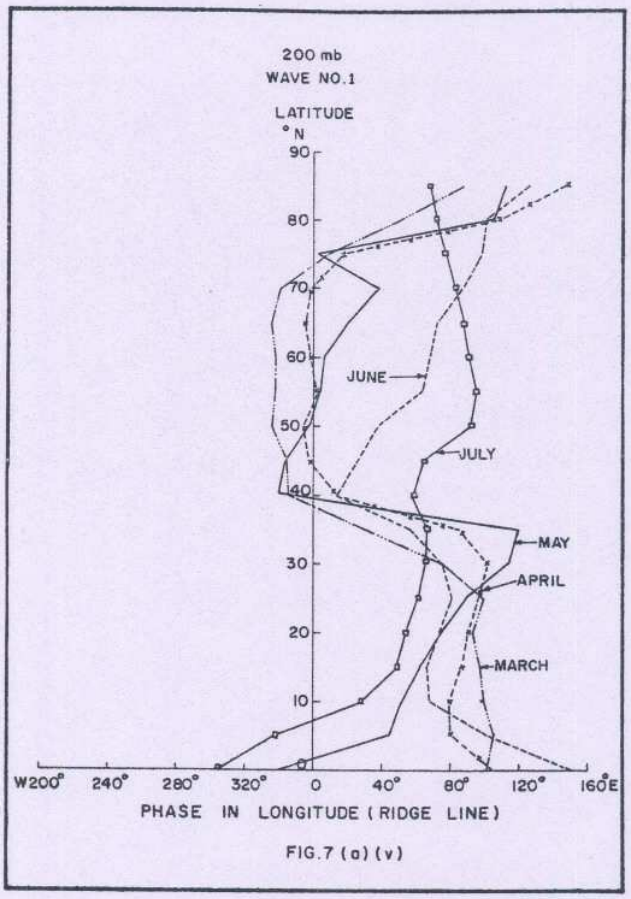

FIG.7 (a) (v)

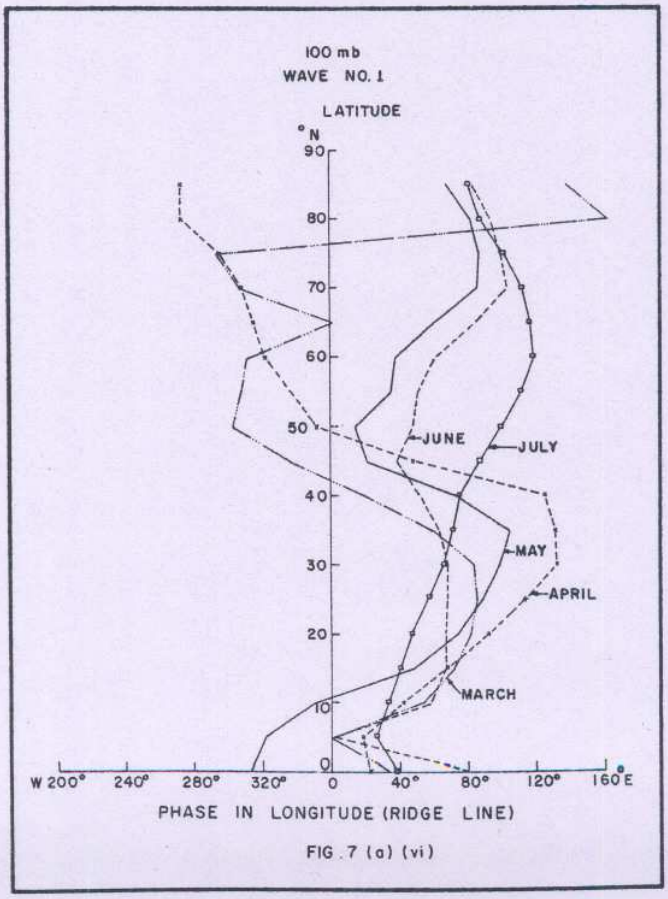

FIG. 7 (a) (vi)

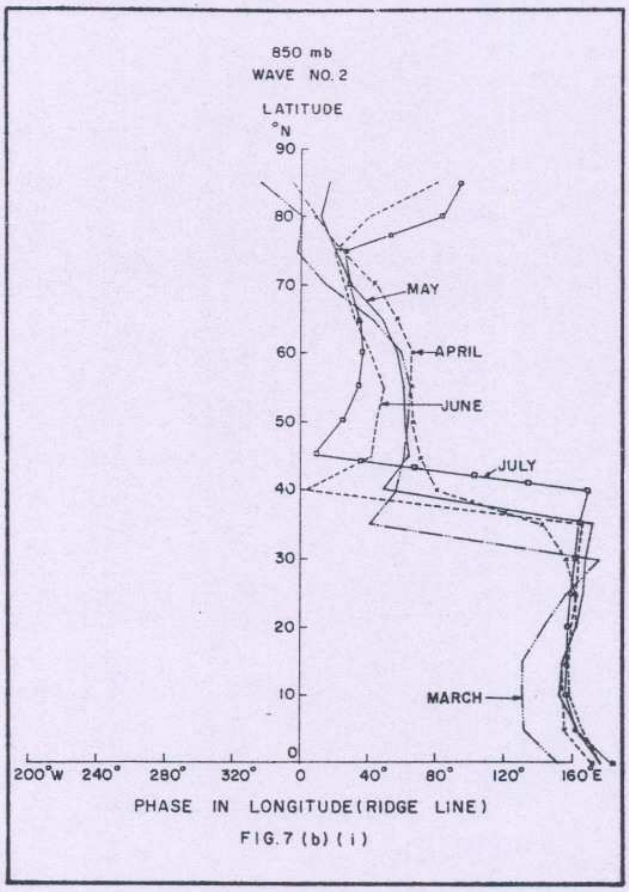

FIG. 7 (b) (i)

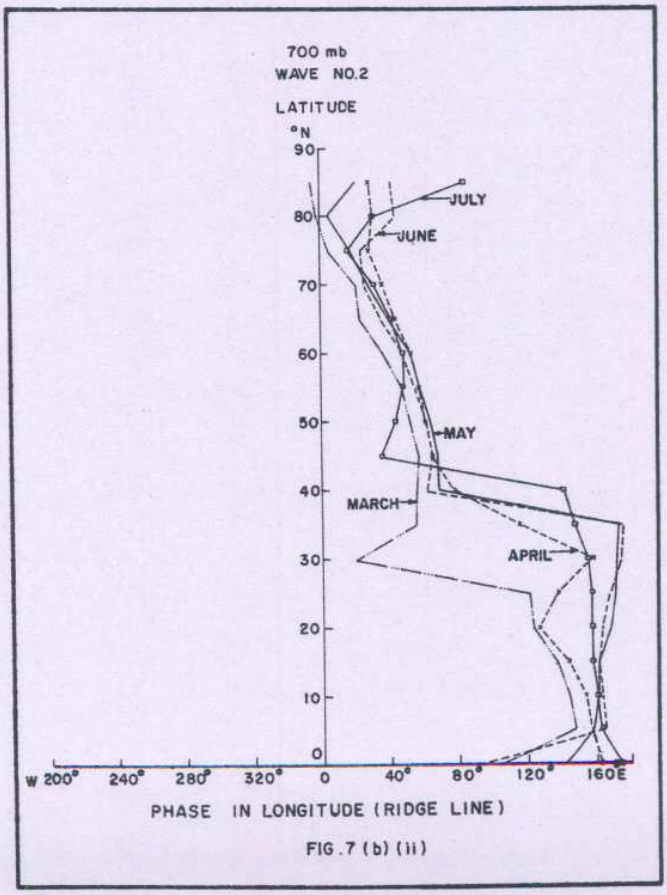

FIG. 7 (b) (ii)

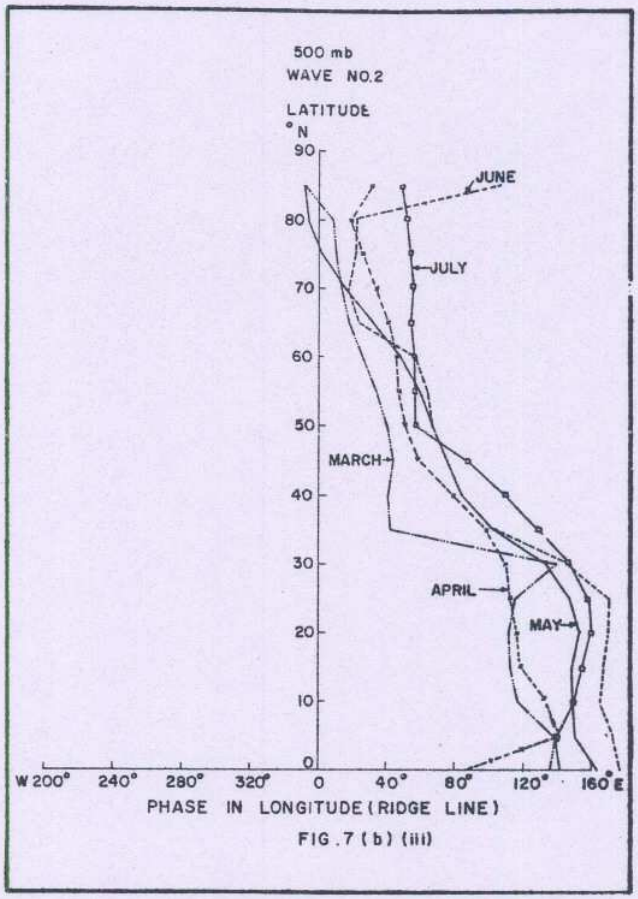

FIG. 7 (b) (iii)

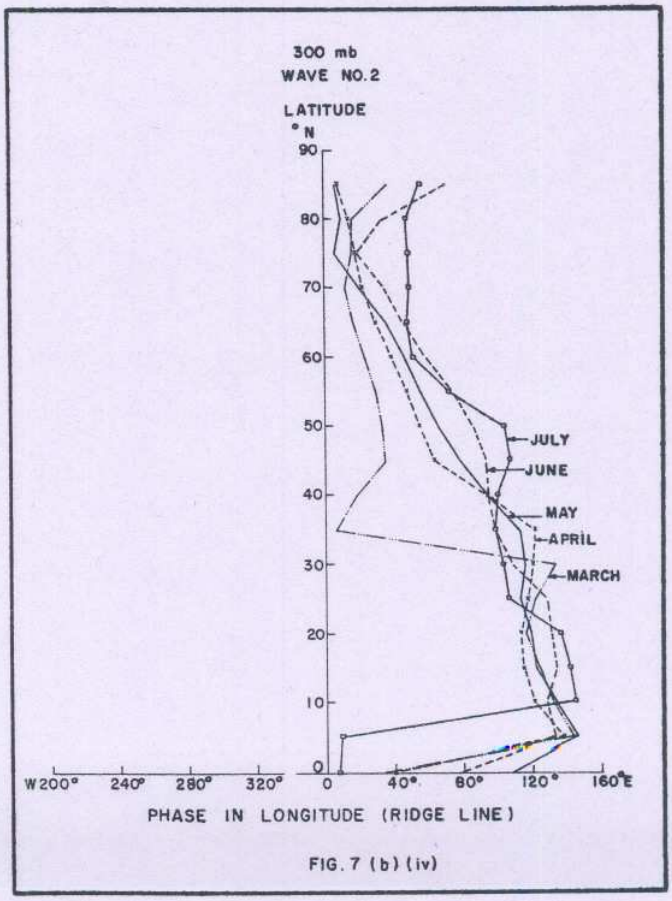

FIG. 7 (b) (iv)

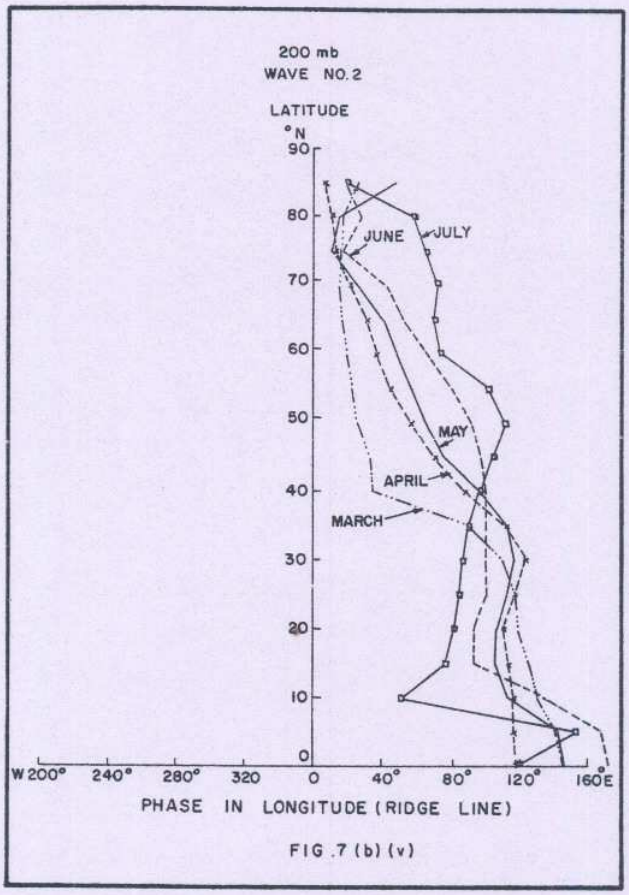

FIG .7 (b) (v)

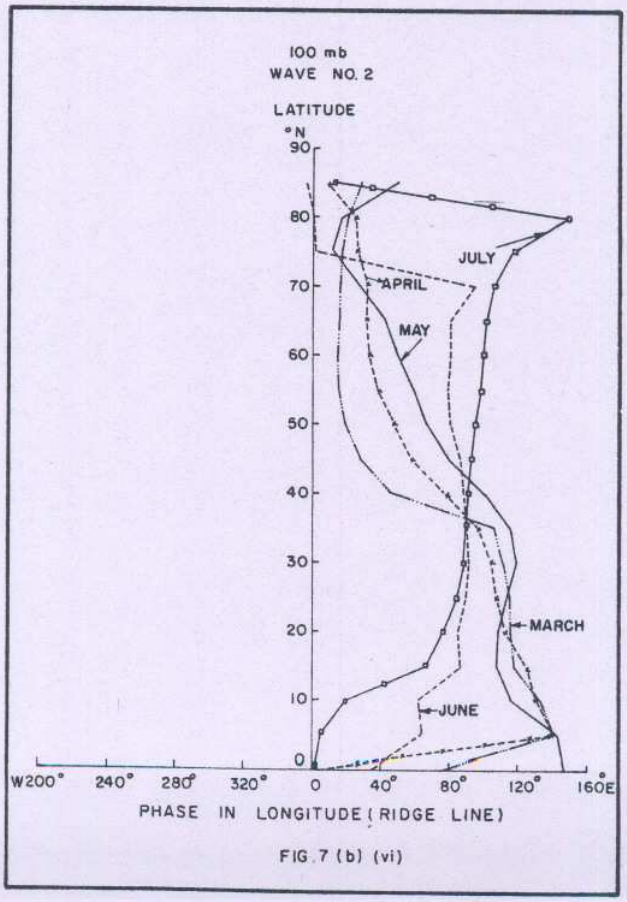

FIG .7 (b) (vi)